https://doi.org/10.5194/egusphere-2023-2318
Preprint. Discussion started: 11 December 2023

Limit analysis of earthquake-induced landslides considering two strength envelopes

Di Wu[1], Yuke Wang[2], Xin Chen[1]

[1]School of Civil Engineering, Suzhou University of Science and Technology, Suzhou, 215129, China
[2]College of Water Conservancy Science and Engineering, Zhengzhou University, Zhengzhou, 450001, China

Correspondence to: Yuke Wang (wangyuke@zzu.edu.cn)

Abstract. Stability analysis of soil slopes undergoing earthquake remains an important research aspect. The earthquake may have some different effects on slope stabilities associated with nonlinear and linear criteria, which need to be further investigated. For homogeneous soil slopes undergoing earthquake, this paper established the three-dimensional (3D) failure mechanisms with the Power-Law strength envelope. The quasi-static method was employed to derive the work rate done by the earthquake in limit analysis theory. The critical heights and critical slip surfaces associated with nonlinear and linear criteria were obtained for four slope examples undergoing different seismic loads. Comparisons of the nonlinear and linear results illustrated that two critical inclinations (resulted from the overlap of nonlinear and linear results) both decrease as the seismic force increases, but their difference is almost constant. For steep slopes, the use of linear strength envelope can lead to the non-negligible overestimation of slope critical height. This overestimation will become significant with the increase of seismic force, especially for the steeper slope with a narrow width. Since the seismic force has positive influence on equivalent internal friction angle, the critical slip surface for the slope obeying nonlinear envelope tends to be slightly deeper as the earthquake becomes stronger. For steep soil slopes undergoing earthquake, the development of 3D stability analysis with nonlinear yield criterion is necessity and significant. These findings can provide some references for risk assessment and landslide disaster reduction of soil slopes.

1 Introduction

Landslide is the classical problem, but it remains to be a hot topic in geotechnical engineering and mining engineering fields. The linear Mohr–Coulomb (MC) failure envelope has universal applications in slope design standards and landside analyses. However, the assumption of linear strength envelope is less rigorous and the curvature of geomaterial strength has been explored by many experimental studies (e.g., Penman, 1953; Bishop et al., 1965; Hoek and Brown, 1980; Maksimovic, 1989; Baker, 2004a). To consider the nonlinear strength behavior of soils, various nonlinear strength criteria have been presented by many researchers (e.g., De Mello, 1977; Zhang and Chen, 1987; Baker, 2004a; Anyaegbunam, 2015; Wang et al., 2023). Meanwhile, a number of scholars successively conducted researches on slope stability analysis using nonlinear strength criteria. Based on the assumptions of slip surfaces and stress distributions, the limit equilibrium methods were widely used to

https://doi.org/10.5194/egusphere-2023-2318
Preprint. Discussion started: 11 December 2023

evaluate the slope safety with nonlinear criteria (Charles and Soares, 1984; Srbulov, 1997; Jiang et al., 2003; Baker, 2004b; Eid, 2010; Deng and Li, 2019; Wan et al., 2023). Besides, some limit analysis approaches with nonlinear strength criteria were conducted to solve slope stability problems by using the tangential method (Drescher and Christopoulos, 1988; Yang and Yin, 2004; Gao et al., 2015; Li and Yang, 2019; Wu et al, 2023). Moreover, several authors employed the numerical methods to analyze the safety of slopes obeying nonlinear criteria (Popescu et al., 2000; Li, 2007; Li and Yang, 2018; Chen and Lin, 2019).

The early work of Charles and Soares (1984) illustrated that the slope safety derived by the linear envelope would be higher than that derived by the nonlinear envelope. Afterwards, numerous authors have paid attention to the distinctions between slope stabilities derived by nonlinear and linear strength envelopes (Srbulov, 1997; Popescu et al., 2000; Jiang et al., 2003; Baker, 2004b; Gao et al., 2015; Li and Yang, 2019). Among them, Baker (2004b) and Gao et al. (2015) compared slope critical heights associated with nonlinear and linear envelopes, and found that using linear envelope could underestimate the stability of slopes in a certain range of inclinations. Gao et al. (2015) further revealed that the linear criterion would derive more significant overestimation or underestimation of slope stability in three-dimensional (3D) conditions. Meanwhile, some attempts have been made to discuss the effects of nonlinear strengths on slip surfaces of two-dimensional (2D) slopes and 3D slopes (Charles and Soares, 1984; Jiang et al., 2003; Wu et al., 2021). It is aware that that the error caused by using linear criterion is not negligible in the assessment of slope safety and the difference between the nonlinear and linear solutions may change for slopes subject to different external influences.

In the field of slope engineering, earthquake is one of the main factors inducing landslide accidents, and numerous investigations have been made to reveal effects of seismic action on the safety of 2D and 3D slopes satisfying linear MC yield criterion. It has been generally accepted that the slope safety will reduce as the seismic action becomes stronger (e.g., Yang et al., 2004; Li et al., 2009; Huang and Ji, 2022). With regard to the influence of earthquake on the rock slope safety, Yang et al. (2004) used the quasi-static method to conduct limit analysis for seismic stability of 2D slopes with Hoek-Brown yield envelope. The limit analysis approach was then carried out by Zhao et al. (2017b) and Pang and Gu (2019) to address seismic stability and seismic displacement of fissured slopes obeying the Hoek–Brown criterion, respectively. Zhong and Yang (2022) presented a modified pseudo-dynamic method to assess seismic stability of 2D slopes by using Hoek–Brown criterion. Allowing for the 3D character of slope geometry, Gao et al. (2016) and Wu et al. (2023) analyzed the seismic stability and the equivalent Mohr–Coulomb parameters for rock slopes with Hoek-Brown envelope in 3D limit analysis framework, respectively. Besides, Li et al. (2009) and Shen and Karakus (2013) performed the numerical methods to assess the slope stability considering nonlinear Hoek-Brown envelope and seismic action in 2D and 3D conditions, respectively. For slopes in soils governed by the nonlinear criterion, Zhao et al. (2017a) focused on the effect of vertical earthquake on the seismic displacement of 2D slopes by using the limit analysis method. Considering the 3D geometry of soil slopes, only the studies of Xu and Yang (2019) and Li and Yang (2019) carried out the limit analysis of seismic stability and seismic displacement of reinforced slopes, respectively. From a general survey of relevant studies, the seismic stability of 3D homogeneous soil slopes with nonlinear criteria remains a lack of research. Especially for soil slopes in 3D condition, few

https://doi.org/10.5194/egusphere-2023-2318
Preprint. Discussion started: 11 December 2023

attempts have been made to illustrate the effect of seismic action on the difference between nonlinear and linear solutions for slope stability.

This paper focused on the influence of earthquake on 3D soil slope stabilities derived by nonlinear and linear strength envelopes. Firstly, the 3D failure mechanisms with the Power-Law strength envelope were developed for soil slopes. Then the quasi-static method was employed to obtain the work rate done by the earthquake and the energy balance equation was established. Afterwards, the optimal upper-bound solutions, in forms of critical height and slip surface, were derived by using an optimization procedure. For several slope examples, the critical heights and slip surfaces associated with nonlinear and linear envelopes were calculated with respect to different slope geometries and seismic actions. The effects of earthquake on nonlinear and linear solutions were discussed on base of presented comparison charts.

2 Limit analysis of 3D slopes undergoing seismic action

2.1 Equivalent MC parameters for nonlinear failure envelope

Among these presented nonlinear strength envelopes, a Power-Law (PL) failure envelope has been applied by many studies to assess slope safety (e.g., Zhang and Chen, 1987; Yang and Yin, 2004; Deng and Yang, 2021; Wu et al, 2023). The PL failure function is presented in the coordinate system of shear stress τ and normal stress σ_n, which is written in the following equation:

$$\tau = c_0\left(1+\frac{\sigma_n}{\sigma_t}\right)^{1/m} \tag{1}$$

in which c_0, σ_t and m are nonlinear strength parameters determined by test data. Figure 1 gives the schematic diagram of PL strength envelope. Parameter σ_t denotes the tensile strength when $\tau = 0$, c_0 is named as the initial cohesion, and m relates to the nonlinearity coefficient with its value bigger than 1.0. When m is equal to 1.0, PL strength function will be reduced to MC yield criterion. Hence, the following slope stability analysis combined with nonlinear strength envelope will contain the solutions for slopes using the linear MC criterion.

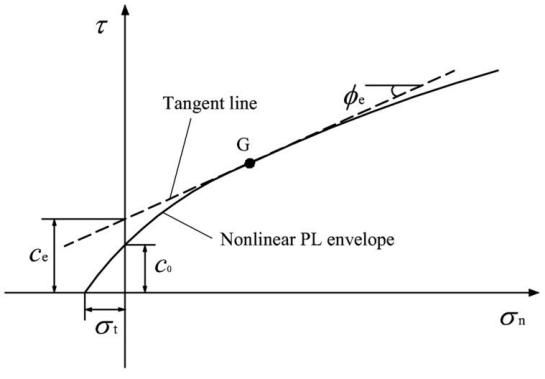

Figure 1: Schematic diagram of PL strength envelope with its tangent line.

https://doi.org/10.5194/egusphere-2023-2318
Preprint. Discussion started: 11 December 2023

As presented in Eq. (1), the friction angle ϕ and the cohesion c will be not constant when the normal stress σ_n is different. This character will result in a big difficult in applying the nonlinear PL failure envelope into the slope stability assessment. Drescher and Christopoulos (1988) firstly addressed such a problem by proposing a tangential technique to simplify the nonlinear strength envelope to an instantaneous linear criterion. This tangential technique was then adopted by some researchers to solve slope safety problems with nonlinear yield criteria (e.g., Yang and Yin, 2004; Zhao et al., 2017a; Pang and Gu, 2019; Deng and Yang, 2021; Wu et al, 2023). These researches gain a certain confidence in the application of tangential technique. A brief description of the tangential technique is presented in Fig. 1. The tangent line function for this curve strength envelope can be presented as follows:

$$\tau = c_e + \sigma_n \tan\phi_e \tag{2}$$

Here, ϕ_e and c_e are the instantaneous strength parameters of tangent line. In this study, they are named as the equivalent friction angle and equivalent cohesion, respectively. Combining the tangent line function and the differential equation $\tan\phi_e = d\tau/d\sigma_n$, the equivalent cohesion c_e can be derived as a function of ϕ_e, which is written as follows:

$$\frac{c_e}{c_0} = \frac{m-1}{m}\left[\frac{\sigma_t}{c_0} m\tan\phi_e\right]^{\left(\frac{1}{1-m}\right)} + \frac{\sigma_t}{c_0}\tan\phi_e \tag{3}$$

In the tangential technique, the tangent line in forms of equivalent shear strengths will be used instead of the PL strength envelope. Hence, the equal or bigger shear strengths will be derived by the tangent line for curve PL envelope in the same σ_n range. Note that the equivalent friction angle ϕ_e will be an optimization variable in the establishment of following limit analysis approach.

2.2 3D failure mechanisms of slopes

For soil slopes obeying MC strength criterion, the 3D failure mechanism presented by Michalowski and Drescher (2009) has been widely applied and further developed in the limit analysis approach (e.g., Gao et al., 2013; Xu and Yang, 2018; Michalowski and Park, 2021; Pan et al., 2023). Considering nonlinear strength behavior of slope soils, Gao et al. (2015) utilized the tangential technique to employ the PL envelope into the modified 3D failure mechanisms of Gao et al. (2013). The 3D kinematic approach was then carried out to further illustrate effects of soil strength nonlinearity on stability assessment of slopes (Gao et al., 2015; Wu et al., 2021). In this study, the modified 3D failure mechanisms combined with nonlinear PL envelope will be similarly adopted to evaluate the stability of homogeneous dry slopes considering seismic actions.

As presented by Gao et al. (2015), the 3D failure mechanisms with nonlinear PL failure envelope should consist of two conditions: the slip surface above slope toe (face failure) and the slip surface below slope toe (base failure). Figures 2 and 3 give two mechanisms of face failure and base failure, respectively. It can be seen that these 3D failure mechanisms are separated by two parts: a curvilinear cone and a plane insertosome. The widths for two parts are $2b'$ and b, and the total slope

https://doi.org/10.5194/egusphere-2023-2318
Preprint. Discussion started: 11 December 2023

width is marked by *B*. The slope height is marked by *H*. In Figs. 2 and 3, an added variable ϕ_e is presented to determine the apex angle for failure mechanism and the tangential line position for the PL envelope. It should be noted that these 3D mechanisms can degrade into the plane-strain 2D mechanism once the relative width *B*/*H* goes infinity. More comprehensive descriptions of these 3D mechanisms can be found in Gao et al. (2013).

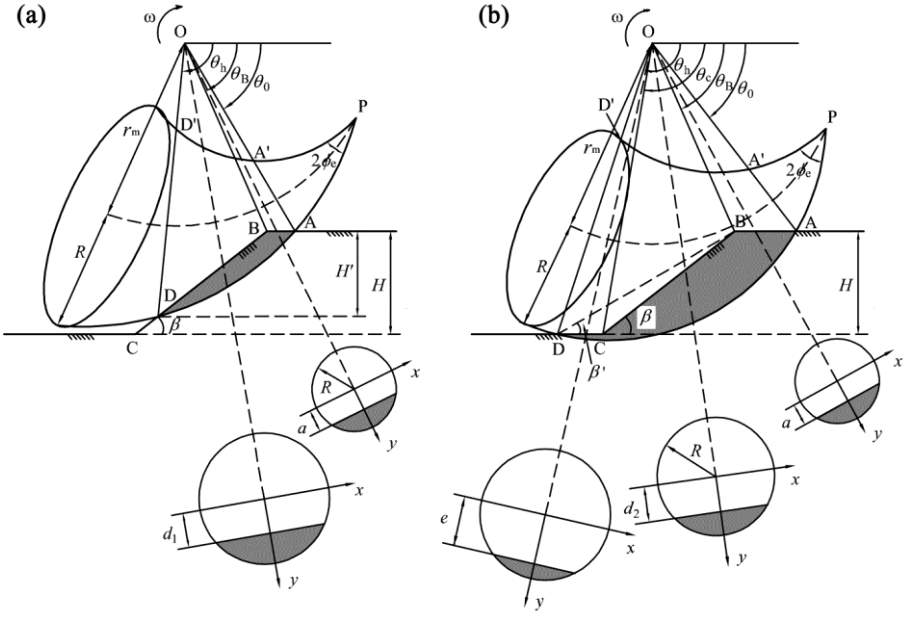

Figure 2: Side view of modified 3D failure mechanisms: (a) face failure; (b) base failure (Gao et al., 2013).

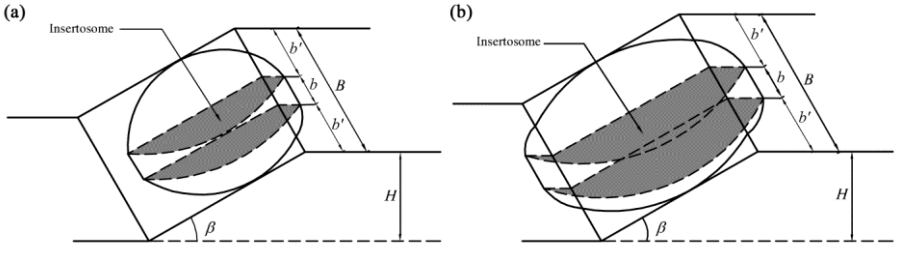

Figure 3: Oblique view of modified 3D failure mechanisms: (a) face failure; (b) base failure (Gao et al., 2013).

2.3 Work rates done by seismic action

To consider the earthquake in the evaluation of slope safety, the quasi-static method is widely applied in the slope stability analysis (e.g., Yang et al., 2004; Li et al., 2009; Pang and Gu, 2019; Huang and Ji, 2022; Wu et al., 2023). In the limit analysis theory, Wu et al. (2023) used the quasi-static method to conduct the seismic stability analysis for rock slopes with a 3D toe failure mechanism. Hence, this paper similarly adopted the quasi-static method to evaluate the seismic load on the modified 3D failure mechanisms of soil slopes. The seismic action can be represented by a horizontal acceleration, which is uniformly distributed in the whole sliding body. Hence, the seismic load is calculated by multiplying the soil self-weight

https://doi.org/10.5194/egusphere-2023-2318
Preprint. Discussion started: 11 December 2023

with the horizontal seismic acceleration coefficient k_h. For the value of seismic acceleration coefficient k_h, this study adopted the range of 0.0 - 0.3.

In the work-energy equation of limit analysis theory, the external work rates consist of two types: self-weight work rate W_γ and horizontal seismic work rate W_s. The work-energy function is established by making these two kinds of external work rates equal to the internal energy dissipation rate D, which has the following expression:

$$W_\gamma^c + W_\gamma^p + W_s^c + W_s^p = D^c + D^p \tag{4}$$

where the superscripts "c" and "p" are used to distinguish the energy rates for curvilinear cone and plane insertosome, respectively. For self-weight work rate W_γ^c and internal energy dissipation rate D^c of curvilinear cone part, see specific expressions in the references of Gao et al. (2013, 2015). The expressions for W_γ^p and D^p of insertosome part can be found in the study of Chen (1975). Due to the application of tangential method, the parameters c and ϕ in these equations need be changed as the equivalent strength parameters c_e and ϕ_e, which have the specific relational expression of Eq. (3). The horizontal seismic work rates W_s are similarly divided into two parts, namely, W_s^c for the curvilinear cone and W_s^p for the plane insertosome.

For 3D face failure mechanism, as shown in Figs. 2(a) and 3(a), the horizontal seismic work rates W_s^c and W_s^p for the curvilinear cone and the plane insertosome are derived by these following expressions:

$$W_s^c = 2\omega k_h \gamma \left[\int_{\theta_0}^{\theta_B} \int_0^{\sqrt{R^2-a^2}} \int_a^{\sqrt{R^2-x^2}} (r_m + y)^2 \sin\theta \mathrm{d}y\mathrm{d}x\mathrm{d}\theta + \int_{\theta_B}^{\theta_h} \int_0^{\sqrt{R^2-d_1^2}} \int_{d_1}^{\sqrt{R^2-x^2}} (r_m + y)^2 \sin\theta \mathrm{d}y\mathrm{d}x\mathrm{d}\theta \right] \tag{5}$$

$$W_s^p = b\omega k_h \gamma r_0^3 (f_{s1} - f_{s2} - f_{s3}) \tag{6}$$

The expressions for the variables a, d_1 and θ_B, and the functions of f_{s1}, f_{s2}, and f_{s3} are listed as follows:

$$a = \frac{\sin\theta_0}{\sin\theta} r_0 - r_m \tag{7}$$

$$d_1 = \frac{\sin(\theta_h + \beta)}{\sin(\theta + \beta)} e^{(\theta_h - \theta_0)\tan\phi_e} r_0 - r_m \tag{8}$$

$$\theta_B = \arctan \frac{\sin\theta_0}{\cos\theta_0 - A'} \tag{9}$$

$$A' = \frac{\sin(\theta_h - \theta_0)}{\sin\theta_h} - \frac{\sin(\theta_h + \beta)}{\sin\theta_h \sin\beta} \left(\sin\theta_h e^{(\theta_h - \theta_0)\tan\phi_e} - \sin\theta_0 \right) \tag{10}$$

$$f_{s1} = \frac{1}{3(1 + 9\tan^2\phi_e)} \left[(3\tan\phi_e \sin\theta_h - \cos\theta_h) e^{3\tan\phi_e(\theta_h - \theta_0)} - 3\tan\phi_e \sin\theta_0 + \cos\theta_0 \right] \tag{11}$$

$$f_{s2} = \frac{1}{3} \frac{l}{r_0} \sin^2\theta_0 \tag{12}$$

https://doi.org/10.5194/egusphere-2023-2318
Preprint. Discussion started: 11 December 2023

$$f_{s3}=\frac{1}{6}e^{\tan\phi_e(\theta_h-\theta_0)}\frac{h}{r_0}\frac{\sin(\theta_h+\beta)}{\sin\beta}\left(2\sin\theta_h e^{\tan\phi_e(\theta_h-\theta_0)}-\frac{h}{r_0}\right) \tag{13}$$

$$\frac{l}{r_0}=\frac{\sin(\theta_h-\theta_0)}{\sin\theta_h}-\frac{\sin(\theta_h+\beta)}{\sin\theta_h\sin\beta}\left[\sin\theta_h e^{\tan\phi_e(\theta_h-\theta_0)}-\sin\theta_0\right] \tag{14}$$

$$\frac{h}{r_0}=\sin\theta_h e^{\tan\phi_e(\theta_h-\theta_0)}-\sin\theta_0 \tag{15}$$

where ω relates to the angular velocity, γ is the soil unit weight, and β represents the slope inclination. As shown in Fig. 2, r_0 and r_0' represent the distances OA and OA′. The other parameters a, d_1, θ_0, θ_B, θ_h, R and r_m have been marked in this figure.

For 3D base failure mechanism (Figs. 2(b) and 3(b)), the seismic work rate done by the slide body below the toe should be added on base of these formulas for 3D face failure mechanism. Hence, these horizontal seismic work rates W_s^c and W_s^p for curvilinear cone and plane insertosome are expressed as the following expressions:

$$W_s^c=2\omega k_h\gamma\left[\int_{\theta_0}^{\theta_B}\int_0^{\sqrt{R^2-a^2}}\int_a^{\sqrt{R^2-x^2}}(r_m+y)^2\sin\theta\,dy\,dx\,d\theta+\int_{\theta_B}^{\theta_C}\int_0^{\sqrt{R^2-d_2^2}}\int_{d_2}^{\sqrt{R^2-x^2}}(r_m+y)^2\sin\theta\,dy\,dx\,d\theta\right.$$
$$\left.+\int_{\theta_C}^{\theta_h}\int_0^{\sqrt{R^2-e^2}}\int_e^{\sqrt{R^2-x^2}}(r_m+y)^2\sin\theta\,dy\,dx\,d\theta\right] \tag{16}$$

$$W_s^p=b\omega k_h\gamma r_0^3(f_{s1}-f_{s2}-f_{s3}-f_{s4}) \tag{17}$$

The relations for these parameters d_2, e and θ_C, and the functions of f_{s1}, f_{s2}, f_{s3}, and f_{s4} can be found from the following equations:

$$d_2=\frac{\sin(\theta_C+\beta)\sin\theta_h}{\sin(\theta+\beta)\sin\theta_C}e^{(\theta_h-\theta_0)\tan\phi_e}r_0-r_m \tag{18}$$

$$e=\frac{\sin\theta_h}{\sin\theta}e^{(\theta_h-\theta_0)\tan\phi_e}r_0-r_m \tag{19}$$

$$\theta_C=\arctan\frac{\sin\theta_h e^{(\theta_h-\theta_0)\tan\phi_e}}{\cos\theta_0-A'-\left(\sin\theta_h e^{(\theta_h-\theta_0)\tan\phi_e}-\sin\theta_0\right)/\tan\beta} \tag{20}$$

$$f_{s1}=\frac{1}{3(1+9\tan^2\phi_e)}\left[(3\tan\phi_e\sin\theta_h-\cos\theta_h)e^{3\tan\phi_e(\theta_h-\theta_0)}-3\tan\phi_e\sin\theta_0+\cos\theta_0\right] \tag{21}$$

$$f_{s2}=\frac{1}{3}\frac{L}{r_0}\sin^2\theta_0 \tag{22}$$

$$f_{s3}=\frac{1}{6}e^{\tan\phi_e(\theta_h-\theta_0)}\frac{H}{r_0}\frac{\sin(\theta_h+\beta')}{\sin\beta'}\left(2\sin\theta_h e^{\tan\phi_e(\theta_h-\theta_0)}-\frac{H}{r_0}\right) \tag{23}$$

https://doi.org/10.5194/egusphere-2023-2318
Preprint. Discussion started: 11 December 2023

$$f_{s4}=\left(\frac{H}{r_0}\right)^2\frac{\sin(\beta-\beta')}{6\sin\beta\sin\beta'}\left[3\sin\theta_h e^{\tan\phi_e(\theta_h-\theta_0)}-\frac{H}{r_0}\right] \tag{24}$$

$$\frac{H}{r_0}=\sin\theta_h e^{\tan\phi_e(\theta_h-\theta_0)}-\sin\theta_0 \tag{25}$$

$$\frac{L}{r_0}=\frac{\sin(\theta_h-\theta_0)}{\sin\theta_h}-\frac{\sin(\theta_h+\beta')}{\sin\theta_h\sin\beta'}\left[\sin\theta_h e^{\tan\phi_e(\theta_h-\theta_0)}-\sin\theta_0\right] \tag{26}$$

in which, the definitions of notations d_2, e, θ_C and β' can be found in Fig. 2(b).

2.4 Determination of upper bound solution

For a given slope with seismic load, the upper bounds of slope stability will be derived by substituting the equations of work rates and internal energy dissipation rates into the work-energy equation. In this study, the upper-bound solutions consist of slope critical height H_{cr} and slip surface. The critical height H_{cr} is the optimized least slope height with the safety factor F_s = 1.0. The expression of H_{cr} can be formulated as follows:

$$H_{cr}=\begin{cases} f\left(\theta_0,\theta_h,\phi_e,r_0'/r_0,b/B,n\right) & \text{3D face-failure mechanism} \\ f\left(\theta_0,\theta_h,\phi_e,r_0'/r_0,b/B,\beta'\right) & \text{3D base-failure mechanism}\end{cases} \tag{27}$$

As shown in Eq. (27), the critical height H_{cr} for face failure mechanism will be calculated in regard to six variables: θ_0, θ_h, ϕ_e, r_0'/r_0, b/B, and $n = H'/H$. Similarly, the critical height H_{cr} for base failure mechanism will be determined in regard to the variables: θ_0, θ_h, ϕ_e, r_0'/r_0, b/B, and β'. The definitions of variables θ_0, θ_h, β', b, B, H', and H can be seen in Figs. 2 and 3. The parameters r_0 and r_0' have been described in the foregoing section. The variable ϕ_e denotes the apex angle of 3D failure mechanism, which will also determine the location of tangent point on nonlinear PL envelope.

To find out the least upper-bound solutions in limit analysis theorem, the optimization procedure of Chen (1992) written in computer codes of MATLAB software was applied in this study. Given the nonlinear and geometric parameters for a slope with certain seismic load, the least values of H_{cr} and corresponding slip surfaces for two failure mechanisms will be both derived by using the optimization procedure. The optimal least upper bound on H_{cr} is the minimum value of two least upper bounds for two failure mechanisms. Meanwhile, the optimal values of the variables (θ_0, θ_h, r_0'/r_0, b/B, n or β', and ϕ_e) will be also determined with respect to the optimal critical height H_{cr}.

For 3D soil slopes obeying the linear MC criterion, the seismic stability solutions can be obtained by using the conversion relationships of $\phi_e = \arctan(c_0/\sigma_t)$ and $c_e = c_0$, which have been addressed in Section 2.1. In the optimization procedure for least upper-bound solutions, the internal friction angle ϕ_e will be a fixed value and it should be removed from the optimization variables.

https://doi.org/10.5194/egusphere-2023-2318
Preprint. Discussion started: 11 December 2023

3 Validation of the research method and presented results

To further validate the rigor of research method and the accuracy of presented results, this section compared the presented results with other studies for two slope examples obeying the linear criterion and the nonlinear criterion, respectively. To facilitate comparison in form of the safety factor F, the shear strength of the nonlinear criterion needs to be divided by F. The reduced shear strength will be used in the presented limit analysis method and the minimum of F can be derived with respect to the least upper bound.

3.1 Comparisons with other linear solutions

For the validation of the accurate linear results derived by this study, the slope example of Gao et al. (2013) was adopted here. For the homogeneous slope, the geometry parameters are given as: B = 20 m, H = 10 m and β = 30°. The slope soil has the properties of c = 40 kPa, ϕ = 15°and γ = 18 kN/m^3. The slope is undergoing both static and seismic actions with k_h = 0.0, 0.1, 0.2, and 0.3. Based on the presented limit analysis method, the minimum safety factor F and the corresponding failure mechanism for this slope example are presented in Table 1. The solutions of Gao et al. (2013) were easily obtained from their given stability charts. It illustrates that the linear solutions derived by this study are in good agreement with the results of Gao et al. (2013). Besides, the failure mechanisms for the slope example under different seismic conditions are also the same for two studies.

Table 1. Comparisons of linear solutions between this study and Gao et al. (2013).

Safety factor F	Horizontal seismic acceleration coefficient k_h			
	0.0	0.1	0.2	0.3
This study	2.77 (toe)	2.29 (toe)	1.94 (base)	1.67 (base)
Gao et al. (2013)	2.77 (toe)	2.30 (toe)	1.93 (base)	1.66 (base)

Note: The result marked by "toe" in the bracket represents that the corresponding slope failure surface passes the toe, and the result marked by "base" represents that the critical failure surface passes the base.

3.2 Comparisons with other nonlinear solutions

The slope problem obeying the nonlinear criterion was adopted from the study of Deng et al. (2015). The nonlinear strength parameters of slope soil are given as follows: c_0 = 29.3 kPa, σ_t = 80.5 kPa, and m = 1.5. The soil unit weight γ is 19.2 kN/m^3. The slope has the height H of 12.2 m and the slope has the inclination β of 26.6°. The slope width is in the range of 40~160m. For this slope example under a static condition, the minimum values of F for slopes with various B/H were calculated and presented in Fig.4. Meanwhile, the limit equilibrium solutions of Deng et al. (2015) were also given in this figure. It can be found that the upper bound solutions obtained in this study are slightly less than the limit equilibrium solutions of Deng et al. (2015), and the maximum difference between them is not more than 5%. Since the slope failure mechanism of Deng et al. (2015) was assumed to be ellipsoid, which seems to be less reasonable than the failure mechanism of this study, the limit

https://doi.org/10.5194/egusphere-2023-2318
Preprint. Discussion started: 11 December 2023

analysis method will derive the slightly smaller safety factor for slopes than the limit equilibrium method. This comparison can further verify the validity of the research method and the accuracy of presented nonlinear results in this study.

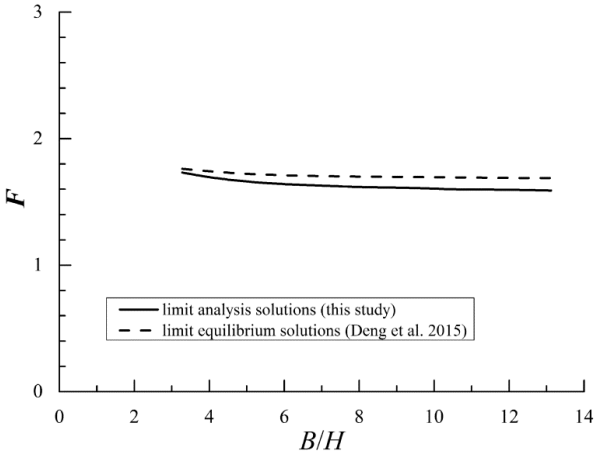

Figure 4: Comparisons of nonlinear solutions between this study and Deng et al. (2015).

4 Computational results and discussions

4.1 Slope examples

To account for the earthquake effect on landslide evaluations using nonlinear and linear strength envelopes, slope examples in four homogenous dry clays were considered in this study. Israeli clay, London clay, Upper Lias clay and Oxford clay were selected as the slope bodies of four slope examples. As illustrated by previous studies (Gao et al., 2015; Wu et al., 2021), the detailed values of the nonlinear and linear strength parameters for these four clays were shown in Table 2. It should be noted that the drainage conditions for these four clays were not consistent in the shear strength tests. Though the total strength parameters derived by undrained strength tests will be appropriate for water-bearing slopes undergoing earthquake, the effective or total strength parameters are both valid for clays in dry conditions. Hence, the nonlinear and linear strength parameters for the four clays can be selected as the soil bodies of slope examples in this study.

Table 2. Soil parameters for four clays.

Four clays	Israeli clay	London clay	Upper Lias clay	Oxford clay
Unit weight γ (kN/m^3)	18.0	18.0	20.0	20.0
c_0 (kPa)	0.06	1.07	0.98	0.16
σ_t (kPa)	0.02	0.15	0.33	0.007
m	1.23	1.66	1.38	1.65
c (kPa)	11.7	6.0	17.0	6.0
ϕ (°)	24.7	32.0	23.0	29.0

https://doi.org/10.5194/egusphere-2023-2318
Preprint. Discussion started: 11 December 2023

4.2 Critical heights of slopes undergoing seismic action

The critical heights for four slopes obeying the nonlinear and linear envelopes were presented in Figs. 5-8 with respect to various width constraints and seismic loads. The sub-graphs (a) – (d) in each figure related to the four conditions of slope example with different width constraints B/H = 1.0, 2.0, 5.0, and ∞ (2D). In these sub-graphs, the critical heights associated with nonlinear criterion (abbreviated as the nonlinear results) were represented by the solid curves and the critical heights associated by linear criterion (abbreviated as the linear results) were represented by the dotted curves. Besides, different color curves represented the critical heights undergoing different seismic loads with k_h = 0.0, 0.1, 0.2, and 0.3.

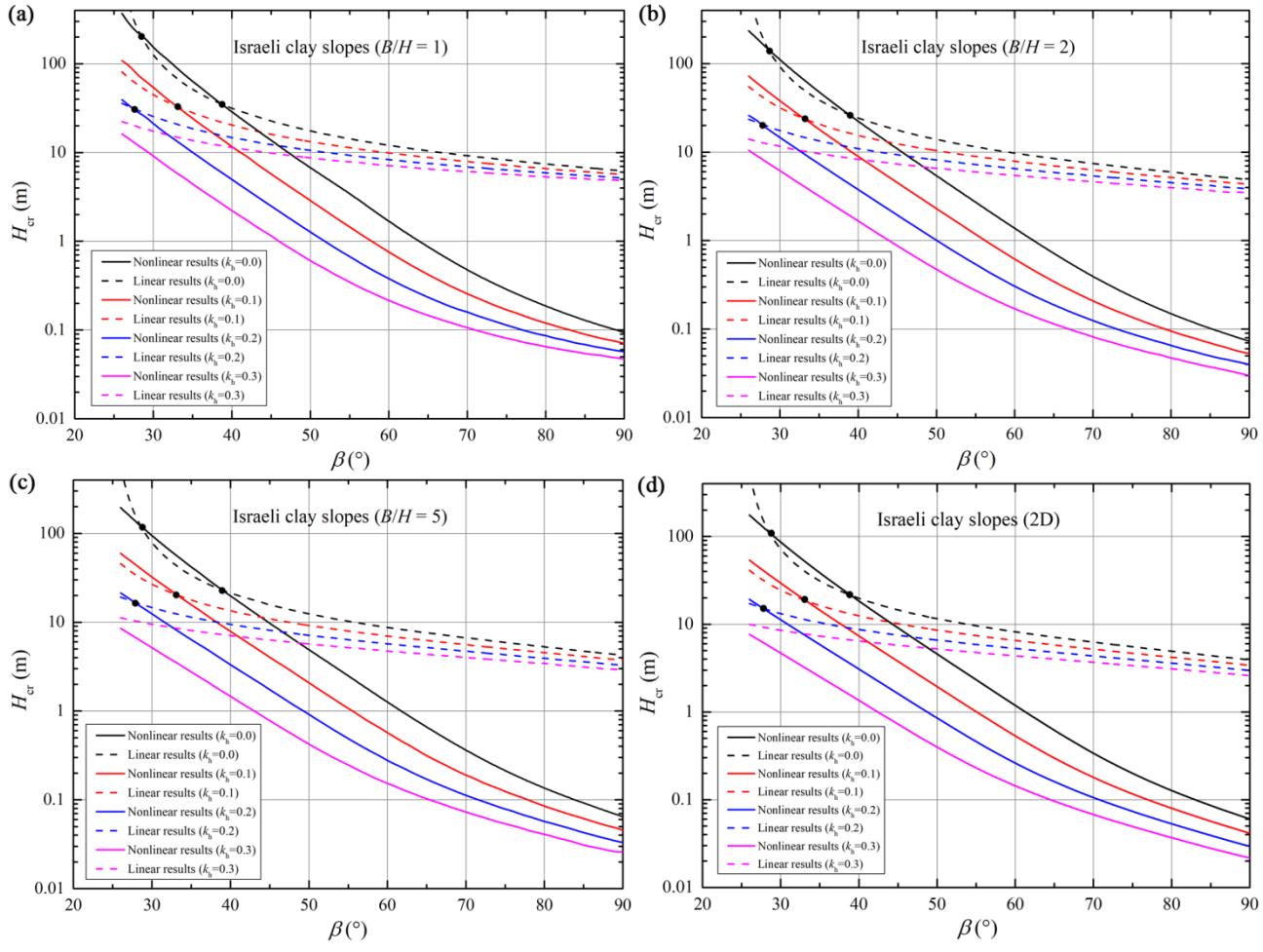

Figure 5: Israeli clay slope critical heights with various k_h.

https://doi.org/10.5194/egusphere-2023-2318
Preprint. Discussion started: 11 December 2023

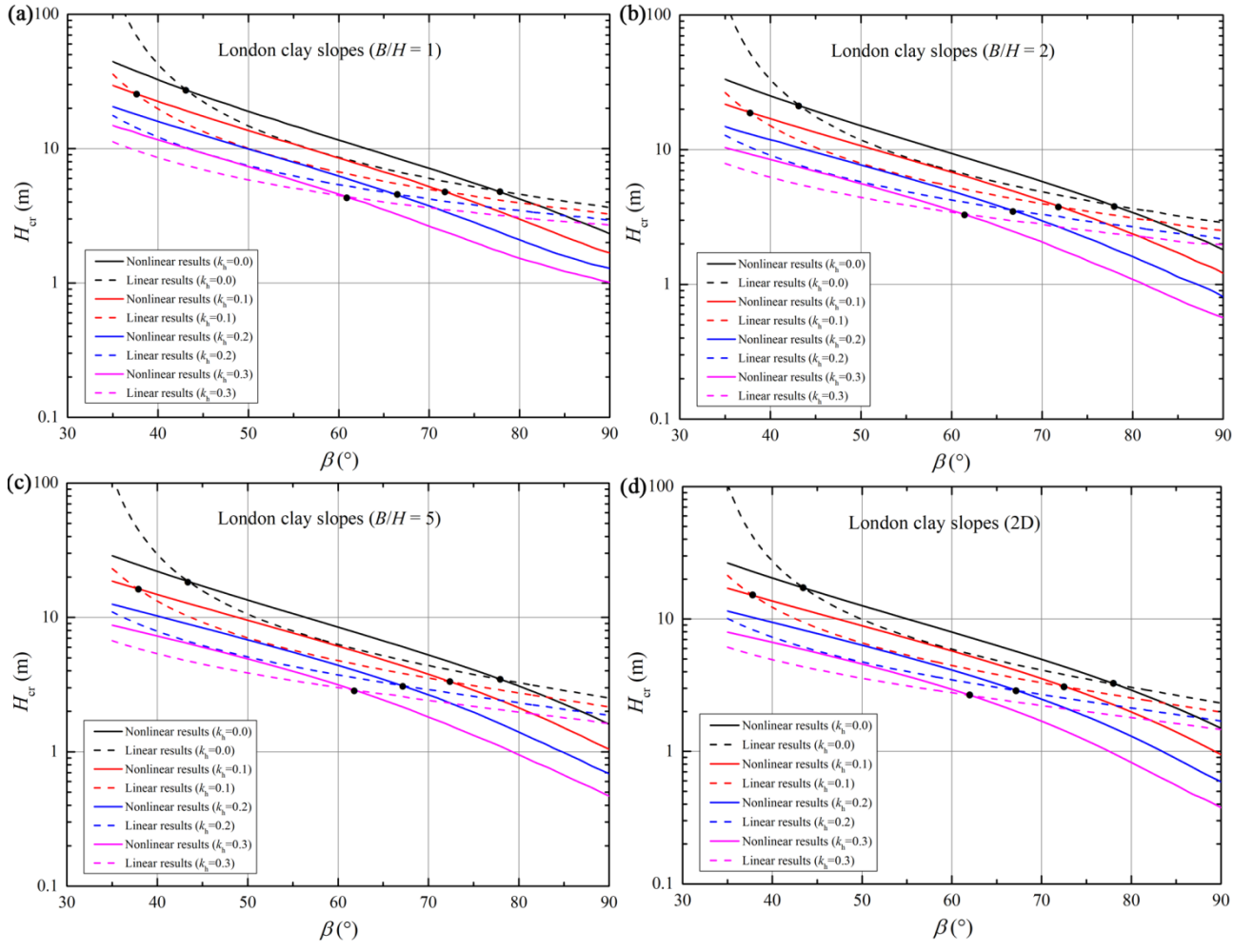

Figure 6: London clay slope critical heights with various k_h.

https://doi.org/10.5194/egusphere-2023-2318
Preprint. Discussion started: 11 December 2023

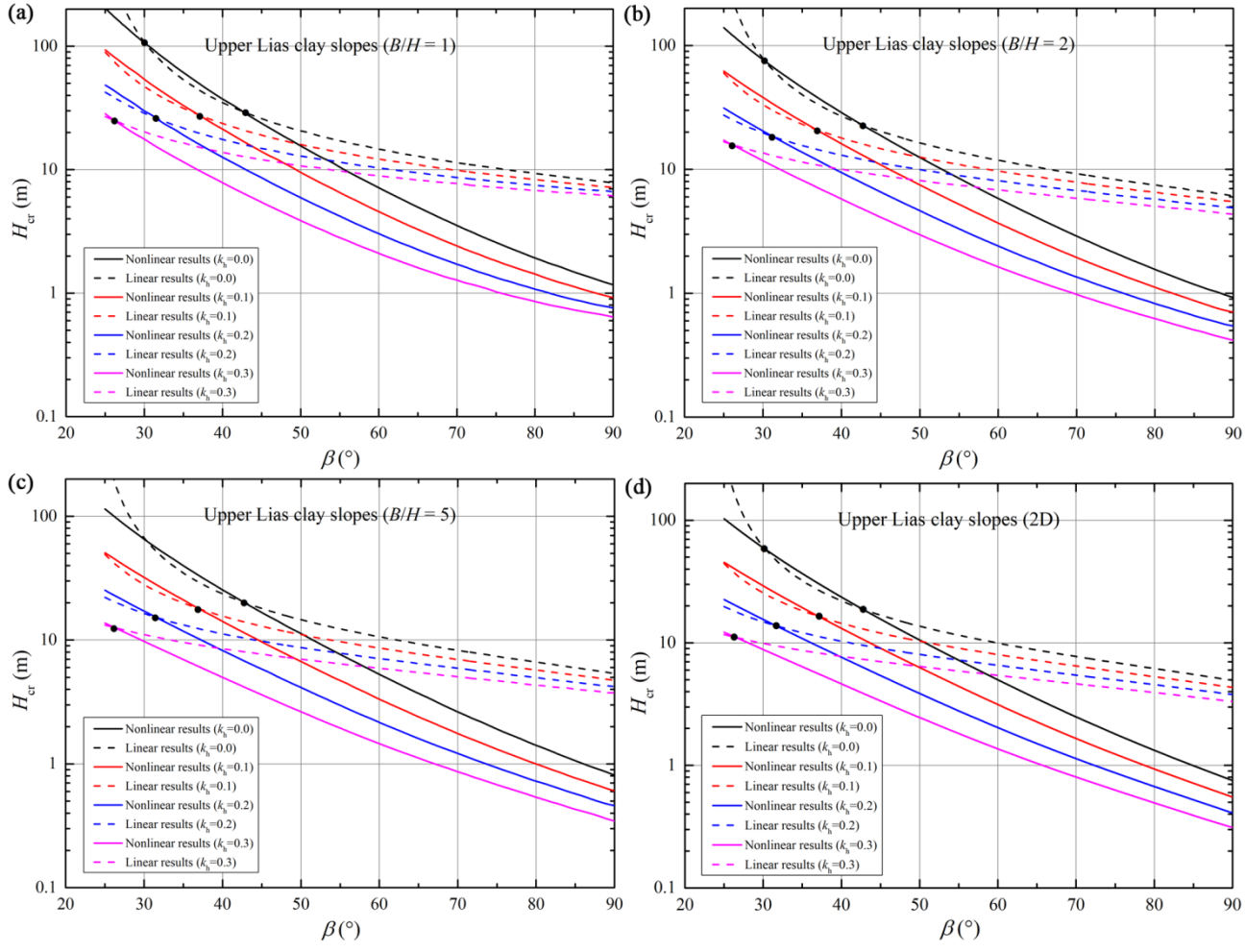

Figure 7: Upper Lias clay slope critical heights with various k_h.

https://doi.org/10.5194/egusphere-2023-2318
Preprint. Discussion started: 11 December 2023

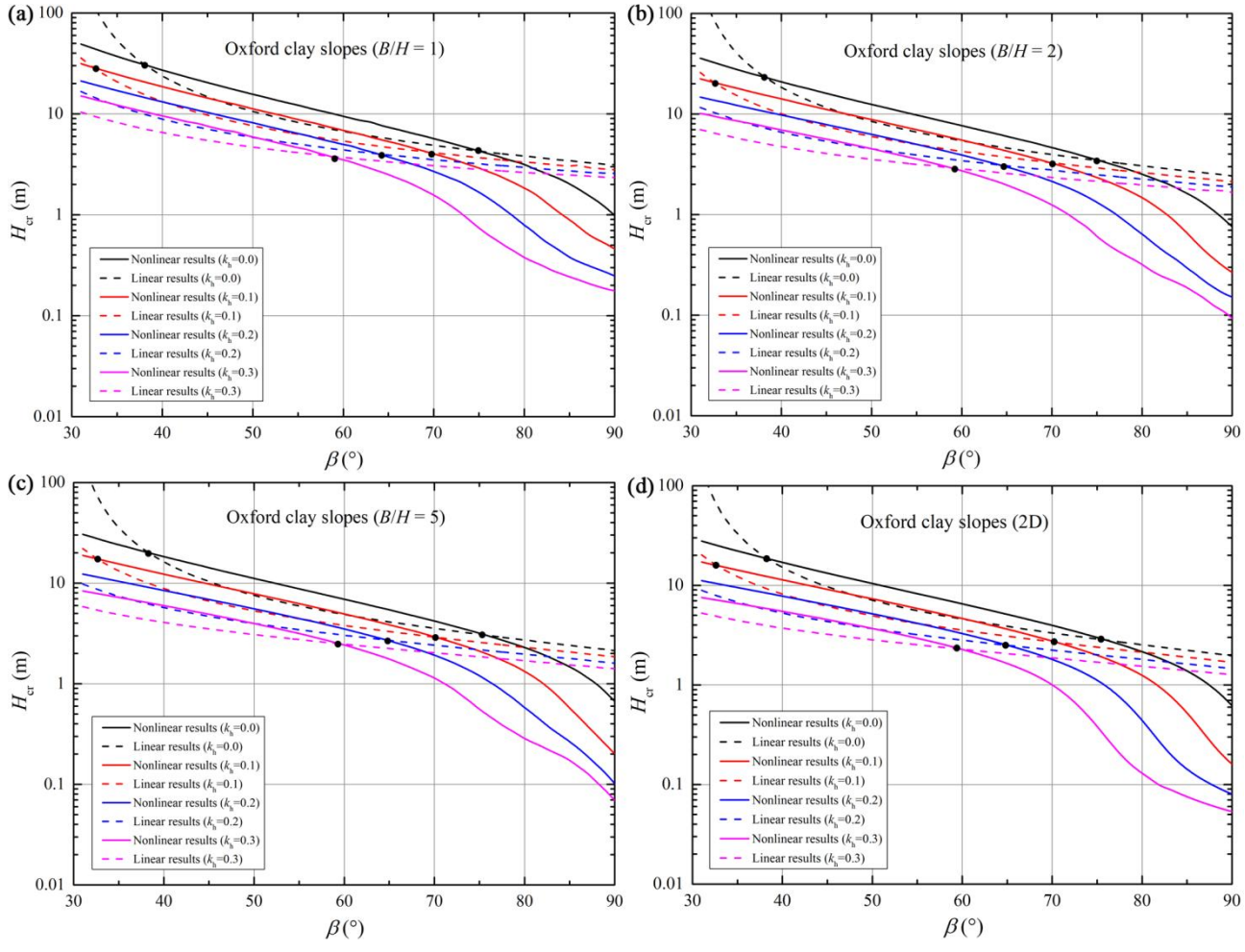

Figure 8: Oxford clay slope critical heights with various k_h.

As illustrated in Figs. 5–8, two critical slope inclinations β_1 (marked by a solid triangle) and β_2 (marked by a solid circle) appear as result of the overlap between nonlinear and linear solutions. For slopes with $\beta_1 < \beta < \beta_2$, the linear solution appears to be higher than the nonlinear one. But for slopes with $\beta < \beta_1$ or $\beta > \beta_2$, using the linear criterion will overestimate the slope critical height and the overestimation cannot be neglected. As illustrated in the previous studies (Baker, 2004b; Gao et al., 2015), two critical slope inclinations are closely related to the overlap of two strength envelopes. For example, when the stability analysis for particular slopes with $\beta_1 < \beta < \beta_2$ is presented by using the nonlinear criterion, the average shear strengths along critical slip surface will be larger than those derived by using the linear criterion. Correspondingly, the nonlinear solution in the form of critical height is larger than the linear one.

The locations of β_1 and β_2 for each slope example will change with the increasing seismic force coefficient k_h. For specific performances, the critical inclination β_1 gradually decreases and the critical inclination β_2 also becomes smaller or vanishes as k_h increases. However, the difference between two critical inclinations β_1 and β_2 seemed to be constant for slopes

https://doi.org/10.5194/egusphere-2023-2318
Preprint. Discussion started: 11 December 2023

with different seismic forces. This finding reveals that the linear solution is a little smaller than the nonlinear solution for gentle slopes undergoing the strong earthquake. For steep slopes obeying the nonlinear PL envelope, the linear MC criterion will derive the bigger critical height and the overestimation will be more significant with the increase of slope inclination. Besides, Figs. 5–8 showed that these distinctions between nonlinear and linear results for slopes with $\beta > \beta_2$ become bigger with an increase of k_h. It may illustrate that using linear MC criterion will more obviously overestimate the critical height of steeper slopes following the nonlinear PL envelope, especially in a case of strong seismic force. Hence, the importance of considering strength nonlinearity in stability analysis seems to be outstanding for steep slopes undergoing strong seismic force.

Meanwhile, Figs. 5–8 also reveal the 3D effects on nonlinear and linear results for four slopes undergoing different seismic loads. It can be observed that the positions of two critical inclinations (β_1 and β_2) tend to be nearly unchanged with an increase in width constraint B/H. But the differences between nonlinear and linear results seem to be smaller as B/H gets bigger. For steeper slopes with stronger seismic load, the ratio of B/H has a more obvious effect on the nonlinear result and then the differences between nonlinear and linear results become significant. This indicates that the application of 3D stability analysis for slopes obeying nonlinear yield criteria is quite necessity, especially for steep slopes with seismic load.

4.3 Slip surfaces of slopes undergoing seismic action

Since 3D effects on slope critical slip surfaces derived by nonlinear and linear envelopes have been well investigated in our foregoing study of Wu et al. (2021), this section chose 2D slopes in Israeli clay and London clay as examples. The influences of seismic load on critical slip surfaces derived by two strength criteria were presented in Figs. 9 and 10 for 2D Israeli clay slopes and 2D London clay slopes. The critical slip surface derived by nonlinear PL envelope (abbreviated as nonlinear slip surface) is represented by the solid line, and the critical slip surface derived by linear MC envelope (abbreviated as linear slip surface) is represented by the dotted line. The critical slip surfaces with various seismic forces are also described by lines in different colors. The four inclinations in sub-graphs (a) – (d) are chose from the ranges of $\beta < \beta_1$, $\beta_1 < \beta < \beta_2$ and $\beta > \beta_2$ for two slopes without seismic load.

https://doi.org/10.5194/egusphere-2023-2318
Preprint. Discussion started: 11 December 2023

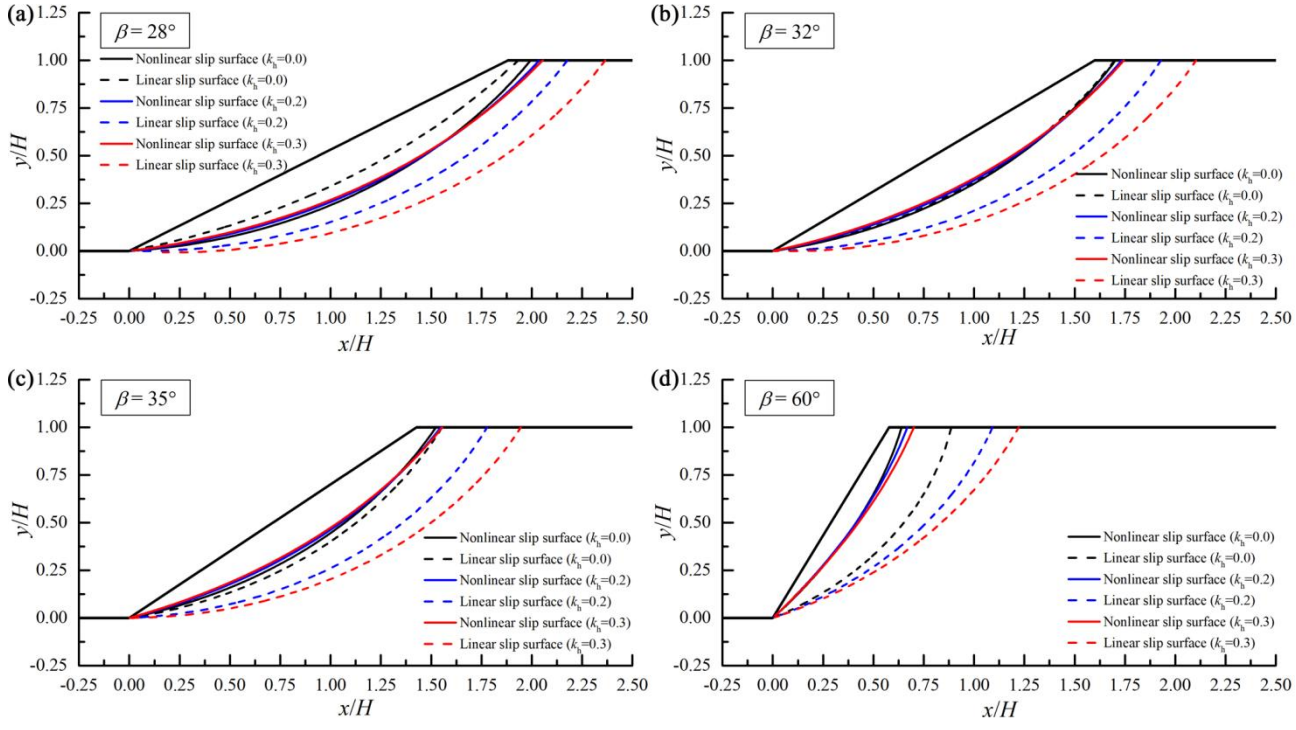

Figure 9: Israeli clay slope slip surfaces with various k_h.

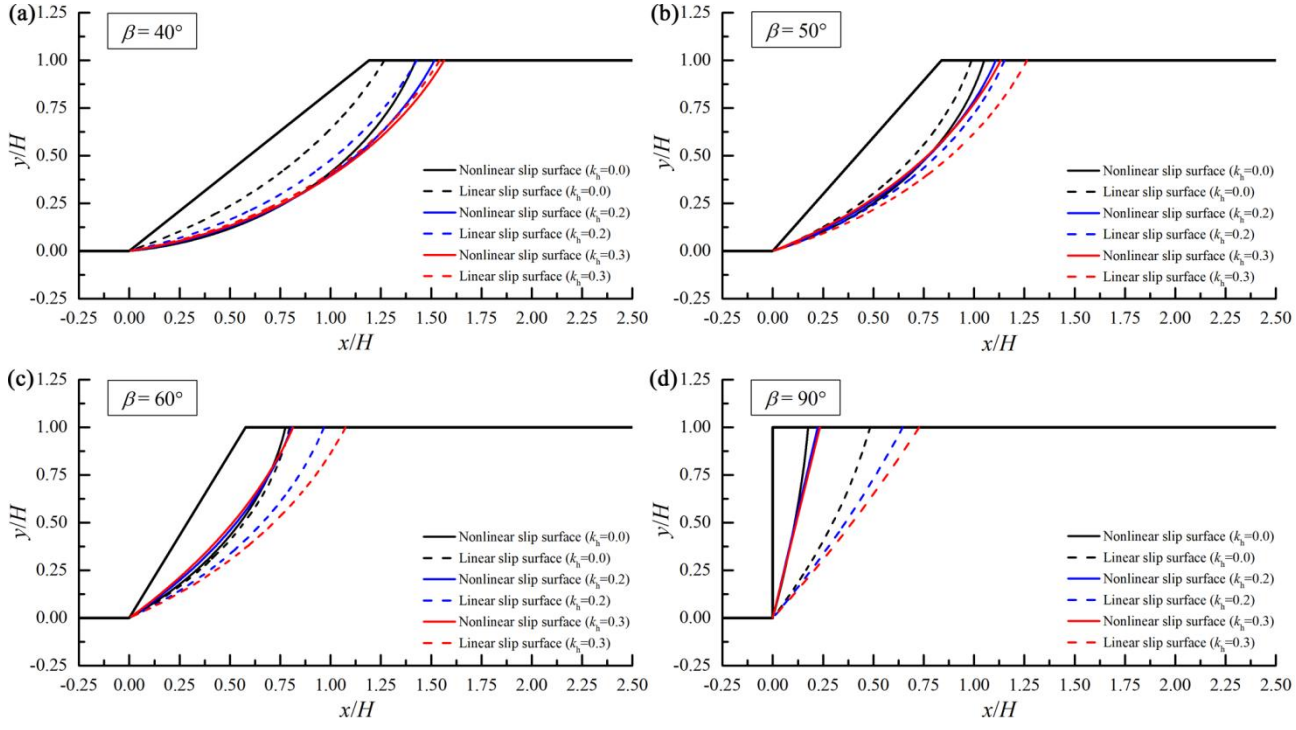

Figure 10: London clay slope slip surfaces with various k_h.

https://doi.org/10.5194/egusphere-2023-2318
Preprint. Discussion started: 11 December 2023

295

As shown in Figs. 9 and 10, for gentle slopes ($\beta < \beta_1$), the linear envelope could derive shallower critical slip surfaces than the nonlinear envelope when the linear average shear strengths are smaller than the nonlinear ones. For slopes with $\beta > \beta_2$, the slope slip surface derived by linear envelope appeared to be deeper than that derived by nonlinear envelope. These findings are similar to the discoveries in the study of Wu et al. (2021), which can be referred to for the specific illustration of
300 above phenomenon.

From Figs. 9 and 10, it can be observed that the influence of seismic load on critical slip surface with nonlinear envelope is different from that on critical slip surface with linear envelope. For slopes with linear envelope, it has been widely accepted that the critical slip surfaces become obviously deeper with an increase in seismic force coefficient k_h. In contrast, the effect of seismic load on critical slip surfaces with nonlinear envelope seemed to be less significant. As the seismic force
305 coefficient k_h becomes bigger, the whole slip surface derived by nonlinear envelope appears to slightly deepen with its starting point farther away from the slope shoulder. Moreover, the effect of seismic force on critical slip surface associated with nonlinear envelope will become less significant for slopes with bigger inclinations.

Above phenomenon may be related to that the equivalent internal friction angle ϕ_e has a variable value affected by the changing seismic load. As illustrated in Fig. 11, the equivalent internal friction angle ϕ_e will get bigger as seismic force
310 coefficient k_h increases. Many previous studies have revealed that the effects of seismic force coefficient k_h and internal friction angle ϕ on slope slip surface location are opposite, namely, the slope slip surface becomes deeper as k_h increases or as ϕ decreases. Hence, considering the influence of ϕ_e on critical slip surface, the slope tends to have a little deeper slip surface with the increasing k_h. It may reveal that k_h has a more significant influence than ϕ_e on critical slip surfaces. Besides, it can be observed from Fig. 11 that the effect of k_h on ϕ_e seems to be less obvious for steep slopes. As a consequence, the
315 seismic load appears to have less obvious effect on critical slip surface of steeper slopes.

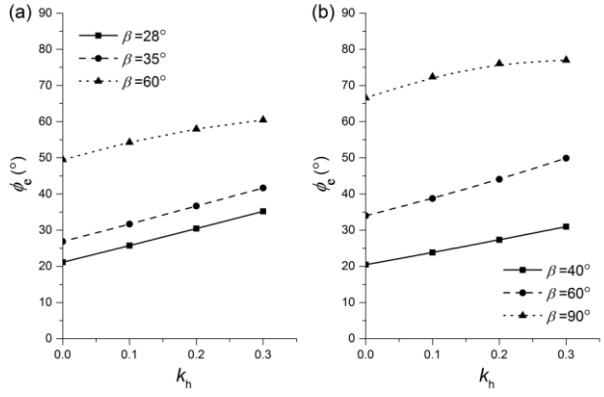

Figure 11: Effect of seismic load on equivalent internal friction angle ϕ_e.

https://doi.org/10.5194/egusphere-2023-2318
Preprint. Discussion started: 11 December 2023

5 Conclusions

In the limit analysis framework, this paper extended an analytic method to assess the stability of 3D soil slopes considering strength nonlinearity and seismic action. The tangential method was used to establish the 3D face failure and 3D base failure mechanisms with the nonlinear PL envelope. The earthquake action was treated as an external seismic force on the failure mechanisms. For a soil slope undergoing the earthquake, the upper-bound solutions in forms of critical height and critical slip surface were derived by using an optimization scheme. The validity of this study was verified by comparisons with other researches. For four clay slope examples, the comparisons of critical heights and slip surfaces associated with nonlinear and linear criteria were presented to illustrate the effects of seismic action on the slope stability evaluations. These results and discussions drew the following conclusions:

(1) As the seismic force increases, two critical inclinations β_1 and β_2 (resulted from the overlap of nonlinear and linear solutions) become smaller or vanish with a constant difference. For gentle slopes undergoing strong seismic force, using linear MC envelope will lead to a little underestimation of the slope critical height. For steep slopes undergoing earthquake, the use of linear MC envelope can pronouncedly overestimate the critical height. Using the nonlinear strength criterion in slope stability analysis is more necessary and significant for soil slopes under earthquake load.

(2) The slope width has slight effect on the positions of two critical inclinations β_1 and β_2 for slopes under seismic action. But the distinctions between nonlinear and linear results become bigger as the slope width becomes smaller. For steeper soil slopes with stronger seismic load, the 3D effect on the slope stability with nonlinear criterion is more obvious.

(3) Compared with the effect of seismic action on linear slip surfaces, the seismic action has a less significant influence on slope slip surfaces derived by nonlinear envelope. When the seismic force becomes bigger, the whole slip surface derived by nonlinear envelope will be a little deeper with its starting point farther away from the slope shoulder. This is related to the fact that equivalent internal friction angle ϕ_e will get bigger with an increase in seismic force.

Data availability

Data is contained with the article or supplementary material.

Author contribution

Di Wu designed the study with contributions from Yuke Wang. Di Wu and Xin Chen performed the data analysis and interpretation. All authors discussed the results. Di Wu prepared the manuscript with contributions from all co-authors.

Competing interests

The authors declare that they have no conflict of interest.

https://doi.org/10.5194/egusphere-2023-2318
Preprint. Discussion started: 11 December 2023

Acknowledgments

This work was sponsored by National Natural Science Foundation of China (Grant Nos. 52178369, 52109140 and 52208361), Natural Science Foundation of the Jiangsu Province Higher Education Institutions of China (Grant No. 23KJB410001) and Natural Science Foundation of Jiangsu Province (Grant No. BK20220638).

References

Anyaegbunam, A.: Nonlinear power-type failure laws for geomaterials: Synthesis from triaxial data, properties, and applications, Int. J. Geomech., 15(1), 04014036, doi: 10.1061/(ASCE)GM.1943-5622.0000348, 2015.

Baker, R.: Nonlinear Mohr envelopes based on triaxial data, J. Geotech. Geoenviron. Eng., 130(5), 498–506, doi:10.1061/(ASCE)1090-0241 (2004)130:5(498), 2004a.

Baker, R.: Stability charts for zero tensile strength Hoek-Brown materials-The variational solution and its engineering implications, Soils Found., 44(3), 125–132, doi:10.1061/(ASCE)1090- 0241(2004)130:5(498), 2004b.

Bishop, A.W., Webb, D.L., and Lewin, P.I.: Undisturbed samples of London clay from the Ashford common shaft: strength–effective stress relationships, Geotechnique, 15(1), 1–31, doi:10.1680/geot.1965.15.1.1, 1965.

Charles, J.A., and Soares, M.: The stability of slopes in soils with nonlinear failure envelopes, Can. Geotech. J., 21 (3), 397–406, doi:10.1139/t84-044, 1984.

Chen, W.F.: Limit analysis and soil plasticity, Amsterdam: Elsevier , 1975.

Chen, Y. and Lin, H.: Consistency analysis of Hoek–Brown and equivalent Mohr–coulomb parameters in calculating slope safety factor, Bull. Eng. Geol. Environ., 78, 4349–4361, doi:10.1007/s10064-018-1418-z, 2019

Chen, Z.Y.: Random trials used in determining global minimum factors of safety of slopes, Can. Geotech. J., 29(2), 225–233, doi:10.1139/t92-026//doi.org/10.1139/t92-026, 1992.

De Mello, V.B.F.: Reflections on design decisions of practical significance to embankment dams: 17th rankine lecture, Geotechnique, 27, 281–354, doi:10.1680/geot.1977.27.3.281, 1977.

Deng, D., Zhao, L., and Li, L.: Limit equilibrium slope stability analysis using the nonlinear strength failure criterion, Can. Geotech. J., 5(52), 563-576, doi:10.1139/cgj-2014-0111, 2015.

Deng, D.P. and Li, L.: Limit equilibrium analysis of slope stability with coupling nonlinear strength criterion and double-strength reduction technique, Int. J. Geomech., 19(6), 04019052, doi:10.1061/(ASCE)GM.1943-5622. 0001431, 2019.

Drescher, A. and Christopoulos, C.: Limit analysis slope stability with nonlinear yield condition, Int. J. Numer. Anal. Methods Geomech., 12(3), 341–345, doi:10.1002/nag.1610120307, 1988.

https://doi.org/10.5194/egusphere-2023-2318
Preprint. Discussion started: 11 December 2023

Eid, H.T.: Two- and three-dimensional analyses of translational slides in soils with nonlinear failure envelopes, Can. Geotech. J., 47(4), 388–399, doi:10.1016/j.enggeo.2013.10.021, 2010.

Gao, Y., Wu, D., Zhang, F., Lei, G.H., Qin, H., and Qiu, Y.: Limit analysis of 3D rock slope stability with non-linear failure criterion, Geomech. Eng., 10(1), 59–76, doi:10.12989/gae.2016.10.1.059, 2016.

Gao, Y., Zhang, F., Lei, G.H., Li, D., Wu, Y., and Zhang, N.: Stability charts for 3D failures of homogeneous slopes, J. Geotech. Geoenviron. Eng., 139(9), 1528-1538, doi:10.1061/(ASCE)GT.1943-5606.0000866, 2013.

Gao, Y., Wu, D., and Zhang, F.: Effects of nonlinear failure criterion on the three-dimensional stability analysis of uniform slopes, Eng. Geol., 198, 87–93, doi:10.1016/j.enggeo.2015.09.010, 2015.

Hoek, E. and Brown, E.T.: Empirical strength criterion for rock masses, J. Geotech. Eng. Division, 106(9), 1013-1035, doi:10.1016/0022-1694(80)90029-3, 1980.

Huang, W. and Ji, J.: Closed-form solutions for regional earthquake–induced landslide prediction: rotational failure mechanism, Landslides, 19(11), 2671-2684, doi:10.1007/s10346-022-01916-5, 2022

Jiang, J.C., Baker, R., and Yamagami, T.: The effect of strength envelope nonlinearity on slope stability computations, Can. Geotech. J., 40(2), 308–325, doi:10.1139/ t02-111, 2003.

Li, A.J., Lyamin, A.V., and Merifield, R.S.: Seismic rock slope stability charts based on limit analysis methods, Comput. Geotech., 36(1–2), 135–148, doi:10.1016/j.compgeo.2008.01.004, 2009.

Li, X.: Finite element analysis of slope stability using a nonlinear failure criterion, Comput. Geotech., 34(3), 127–136, doi:10.1016/j.compgeo.2006.11.005, 2007.

Li, Y. and Yang, X.: Seismic displacement of 3D slope reinforced by piles with nonlinear failure criterion, Int. J. Geomech., 19(6), 04019042, doi:10.1061/ (ASCE)GM.1943-5622.0001411, 2019.

Li, Y.X. and Yang, X.L.: Soil-slope stability considering effect of soil-strength nonlinearity, Int. J. Geomech., 19(3), 04018201, doi:10.1061/(ASCE)GM. 1943-5622.0001355, 2018.

Maksimovic, M.: Nonlinear failure envelope for soils, J. Geotech. Eng., 115(4), 581–586, doi:10.1061/(ASCE)0733-9410(1989)115:4(581), 1989.

Michalowski, R.L. and Drescher, A.: Three-dimensional stability of slopes and excavations, Geotechnique, 59(10), 839-850, doi:10.1680/geot.8.P.136, 2009.

Michalowski, R.L. and Park, D.: Three-dimensional ridge collapse mechanism for narrow soil slopes, Int. J. Numer. Anal. Methods Geomech., 45(13), 1972-1987, doi:10.1029/JC084iC01p00338, 2021.

https://doi.org/10.5194/egusphere-2023-2318
Preprint. Discussion started: 11 December 2023

Pan, Q., Zhang, R., Wang, S., Chen, J., Zhang, B., Zou, J., and Yang, X.: Three-dimensional stability of slopes under water drawdown conditions, Int. J. Geomech., 23(1), 04022254, doi:10.1061/(ASCE)GM.1943-5622.0002614, 2023.

Pang, Z. and Gu, D.: Seismic stability of a fissured slope based on nonlinear failure criterion, Geotech. Geol. Eng., 37(4), 3487–3496, doi:10.1007/s10706-019-00806-3, 2019.

Penman, A.: Shear characteristics of saturated silt measured in triaxial compression, Geotechnique, 3(8), 312–328, doi:10.1680/geot.1953.3.8.312, 1953.

Popescu, M., Ugai, K., and Trandafir, A.: Linear versus nonlinear failure envelopes in LEM and FEM slope stability analysis, Proc. 8th Int. Symp. on Landslides, 3, 1227–1234, 2000.

Shen, J. and Karakus, M.: Three-dimensional numerical analysis for rock slope stability using shear strength reduction method, Can. Geotech. J., 51(2), 164–172, doi:10.1139/cgj-2013-0191, 2013.

Srbulov, M.: On the influence of soil strength brittleness and nonlinearity on slope stability, Comput. Geotech., 20(1), 95–104, doi:10.1016/S0266-352X (96) 00014-6, 1997.

Wan, Y., Gao, X., Wu, D., and Zhu, L.: Reliability of spatially variable soil slope based on nonlinear failure criterion, Nat. Hazards, 117(1), 1179-1189, doi:10.1007/s11069-023-05868-4, 2023.

Wang, Z., Pan, P., Zuo, J., and Gao, Y.: A generalized nonlinear three-dimensional failure criterion based on fracture mechanics, J. Rock Mech. Geotech. Eng., 15(3), 630-640, doi:10.1016/j.jrmge.2022.05.006, 2023.

Wu, D., Chen, X., Tao, Y., and Meng, X.: Estimating Mohr–Coulomb strength parameters from the Hoek–Brown criterion for rock slopes undergoing earthquake, Sustain., 15(6), 5405, doi:10.3390/su15065405, 2023.

Wu, D., Gao, Y., Chen, X., and Wang, Y.: Effects of soil strength nonlinearity on slip surfaces of homogeneous slopes, Int. J. Geomech., 21(1), 06020035, doi:10.1061/(ASCE)GM.1943-5622.0001896, 2021.

Xu, J. and Yang, X.: Seismic stability of 3D soil slope reinforced by geosynthetic with nonlinear failure criterion, Soil Dyn. Earthq. Eng., 118, 86–97, doi:10.1016/j.soildyn.2018.12.019, 2019.

Xu, J.S. and Yang, X.L.: Three-dimensional stability analysis of slope in unsaturated soils considering strength nonlinearity under water drawdown, Eng, Geol., 237, 102-115, doi:10.1016/j.enggeo.2018.02.010, 2018.

Yang, X.L., Li, L., and Yin, J.H.: Seismic and static stability analysis for rock slopes by a kinematical approach, Geotechnique, 54(8), 543–550, doi:10.1680/geot.2004.54.8.543, 2004.

Yang, X.L. and Yin, J.H.: Slope stability analysis with nonlinear failure criterion, J. Eng. Mech., 130(3), 267–273, doi:10.1061/(ASCE)0733-9399(2004)130: 3(267) , 2004.

https://doi.org/10.5194/egusphere-2023-2318
Preprint. Discussion started: 11 December 2023

Zhang, X.J. and Chen, W.F.: Stability analysis of slopes with general nonlinear failure criterion, Int. J. Numer. Anal. Methods Geomech., 11(1), 33–50, doi:10.1002/ nag.1610110104, 1987.

Zhao, L., Cheng, X., Dan, H., Tang, Z., and Zhang, Y.: Effect of the vertical earthquake component on permanent seismic displacement of soil slopes based on the nonlinear Mohr–Coulomb failure criterion, Soils Found., 57(2), 237-251, doi:10.1016/j.sandf.2016.12.002 , 2017a.

Zhao, L., Cheng, X., Li, L., Chen, J., and Zhang, Y.: Seismic displacement along a log-spiral failure surface with crack using rock Hoek–Brown failure criterion, Soil. Dyn. Earthq. Eng., 99, 74–85, doi:10. 1016/ j.sandf.2016.12.002, 2017b.

Zhong, J.H. and Yang, X.L..: Pseudo-dynamic stability of rock slope considering Hoek–Brown strength criterion, Acta Geotech., 17, 2481–2494, doi:10.1007/s11440-021-01425-0, 2022.